Original Article

sciendo

Non-invasive evaluation of fluid dynamic of aortoiliac atherosclerotic disease: Impact of bifurcation angle and different stent configurations

Gianluca Rigatelli[1], Marco Zuin[2], Fabio Dell'Avvocata[1], Aravinda Nanjundappa[3], Ramesh Daggubati[4], Thach Nguyen[5]

[1]Section of Cardiovascular Diagnosis and Endoluminal Interventions, Rovigo General Hospital, Rovigo, Italy;
[2]Department of Cardiology, Rovigo General Hospital, Rovigo, Italy;
[3]Department of Surgery, West Virginia University School of Medicine, Morgantown, WV, USA;
[4]Head, Cardiac Catheterization Laboratories, Winthrop University Hospital Mineola, NY, USA;
[5]Cardiovascular Research, Methodist Hospital, Merrillville, IN, USA; Tan Tao University, School of Medicine, Tan Duce City, Long An, Vietnam

ABSTRACT

Objectives: To non-invasively evaluate by computational fluid dynamic (CFD) analysis the physiology and rheology of aortoiliac bifurcation disease at different angles and different stent configurations. **Material and Methods:** For the analysis, we considered a physiologic model of abdominal aorta with an iliac bifurcation set at 30°, 45° and 70° without stenosis. Subsequently, a bilateral ostial common iliac stenosis of 80% was considered for each type of bifurcation. For the stent simulation, we reconstructed Zilver vascular self-expanding (Zilver; Cook, Bloomington, MN) and Palmaz Genesis Peripheral (Cordis, Miami, FL) stents. **Results:** The physiologic model, across the different angles, static pressure, Reynolds number and stream function, were lower for the 30° bifurcation angle with a gradient from 70° to 30° angles, whereas all the other parameters were inversely higher. After stenting, all the fluid parameters decreased homogenously independent of the stent type, maintaining a gradient in favour of 30° compared to 45° and 70° angles. The absolute greater deviation from physiology was observed for low kissing when self-expandable stents were used across all angles; in particular, the wall shear stress was high at at 45° angle. **Conclusion:** Bifurcation angle deeply impacts the physiology of aortoiliac bifurcations, which are used to predict the fluid dynamic profile after stenting. CFD, having the potential to be derived both from computed tomography scan or invasive angiography, appears to be an ideal tool to predict fluid dynamic profile before and after stenting in aortoiliac bifurcation.

Key words: iliac artery, stenting techniques, computational fluid dynamic, endovascular

Address for Correspondence:
Dr. Gianluca Rigatelli, MD, PhD, EBIR, FACP, FACC, FESC, FSCAI, Cardiovascular Diagnosis and Endoluminal Interventions, Rovigo General Hospital, 45100 Rovigo, Italy.
E-mail: jackyheart71@yahoo.it

Access this article online
Website: www.intern-med.com
DOI: 10.2478/jtim-2018-0020
Quick Response Code:

INTRODUCTION

Aortoiliac bifurcation has been extensively evaluated in the past in atherosclerotic disease amenable to both surgical and interventional repair.[1-2] The impact of different bifurcation angles and different stent types and configurations has not been clarified yet. Computational fluid dynamics (CFD) has been recently widely applied in many fields of cardiovascular medicine,[3] providing important information about physiology of the cardiovascular system, and because of its ability to predict the results of interventional techniques applied to the cardiovascular system.[4]

The aim of the present study is to evaluate by computational fluid dynamic (CFD) analysis the physiology of the aortoiliac bifurcation at different angles and the impact of different stent types and configurations on its rheology.

MATERIAL AND METHODS

Aortic bifurcation

In our analysis, we considered three different hypothetic models of aortic bifurcation, taking also into account the different aortic-iliac take-off angles.[1] In particular, we considered three different aortic angles (α): 30°, 45° and 70°. These carrefour's angles have been selected on the basis of our retrospective evaluation of our institutional database of 1556 patients (mean age 76.7±14.8, 681 females) who underwent abdominal aorta angiography in the last 5 years from 1 January 2011 to 1 January 2016. In particular, aortic bifurcations were measured using an electronic goniometer after performing diagnostic angiography. Angles were represented as follows: 682 patients (43.8%) presented an angle of approximately 45° (39°–58°), 590 patients (37.9%) an angle approximately 30° (<30°–38°) and 284 (18.2%) and angle approximately 70° (59°–>70°). Left iliac artery had a different and smaller angle compared to right iliac artery in only 390 (25.1%) of the patients and the difference was only of 12±8.4°. So this difference has been not accounted for in the model. A schematic representation of the geometry is given in Figure 1. In particular, the diameter of the aorta has been set to 25 mm while the diameter of distal iliac arteries has been set to 9 mm. The length and percentage of artery occlusion provoked by the atherosclerotic plaques have been set to 40 mm and 80%, respectively. To simplify the model, arteries were assumed to be simple cylinders. Moreover, the *X*-axis was considered to be a symmetric axis. The model was constructed using Rhinoceros v. 4.0 Evaluation (McNeel & Associates, Indianapolis, IN).

Stent simulation

For stent simulation, we reconstructed the strut design and linkage pattern of two different types of stents: Zilver vascular self-expanding stent (Zilver; Cook, Bloomington, MN, USA) and Palmaz Genesis peripheral stent (Cordis, Miami, FL), which are routinely used in our institution. Computer-aided design (CAD) software was used to reproduce the stent geometry as accurate as possible (SolidWorks 2009, Solidworks Corp, Conconr, MA). In the first step, we created the solid model of aorta bifurcation and then the expanded stent geometry. For this purpose, a hollow tube with outer diameter equal to both the nominal expanded diameter and thickness of the stent was created. Then, a two-dimensional sketch with the stent's strut was propagated and wrapped around the tube. Through a cut-out, the obtained ring of the stent was propagated axially to create the full-length, expanded model. In our models, the artery walls and plaque components were assumed to be isotropic, linear and elastic with a constant Young's modulus (*E*), density and Poisson's ratio. For stent simulation, devices were modelled as a shell-type tube; the mechanical properties such as density and Poisson's ratio were in accordance with the reported technical properties of the stent. The arterial wall thickness was considered to be constant at 0.5 mm. A 3-D reconstruction of the stents is given in Figure 2.

Virtual implantation

After the stent model was placed in the correct position, according to the different stenting techniques, material removal, depending on the considered techniques, was applied. Subsequently, using Boolean operation, the

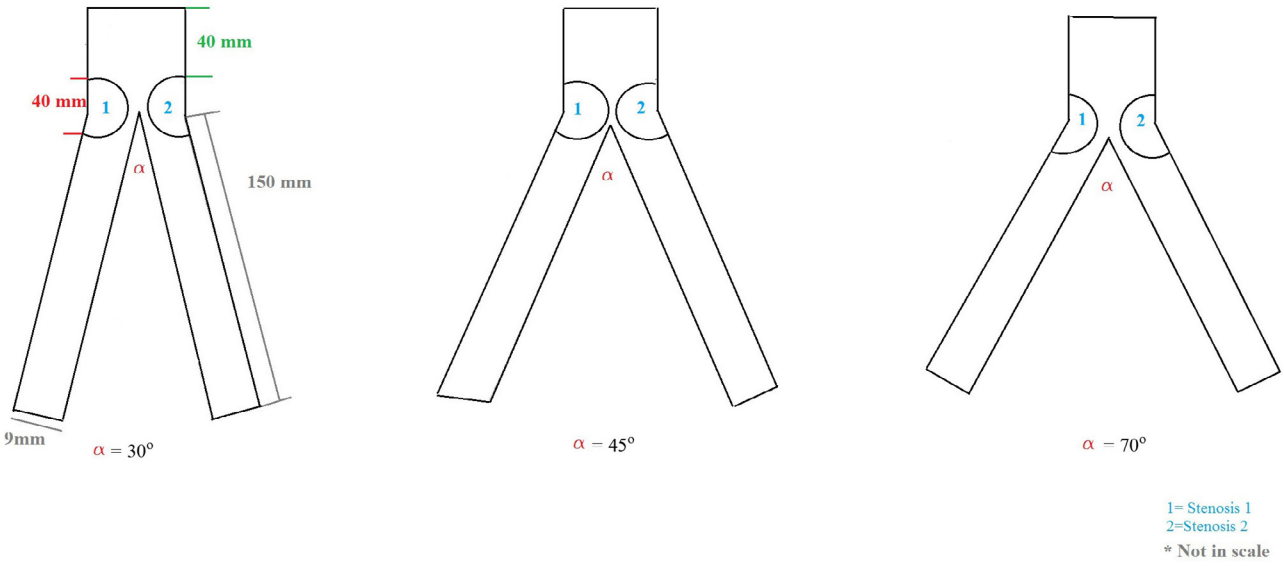

Figure 1: Schematic representation of the aortic Carrefour showing the considered angles and the fixed stenosis.

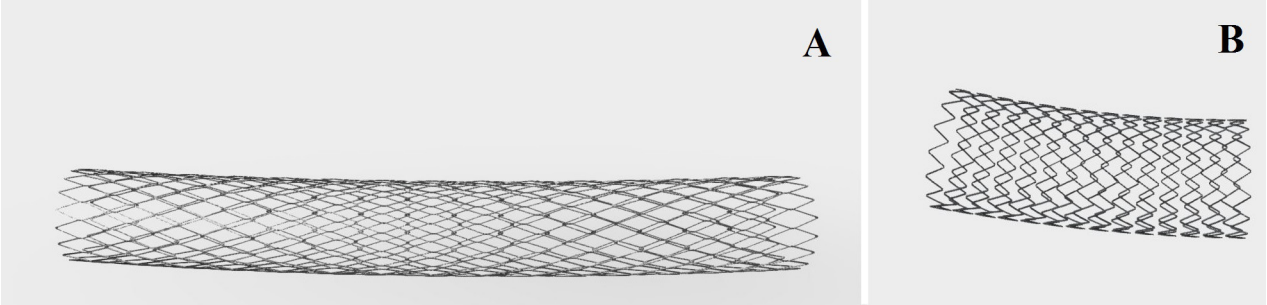

Figure 2: 3D reconstruction of stents used in the CDF analysis. A: Palmaz genesis peripheral stent; B: Cook-Zilver vascular self-expanding stent.

modified solid model is subtracted from the bifurcation model to obtain the final geometry. In particular, we assumed that after stent deployment and implantation, both in the aorta and both iliac arteries, there were no residual stenosis. We used two different types of kissing: high kissing and low Kissing (Figure 2). Implantation technique used in the model included (1) predilation of both common iliac arteries with a 7.0 × 40 balloon at nominal pressure (10 atm), (2) kissing stent implantation in both common iliac arteries of a 1:1 stent with respect to the vessel diameter (balloon expandable at 14 atm or self-expandable), and finally (3) post-dilation with a balloon 9.0 × 40 balloon at 14 atm.

CFD analysis

The fluid type applied in the simulation is a non-Newtonian fluid. For simulation purposes, a steady-state (*i.e.*, non-pulsatile) laminar blood flow was assumed, where the inlet pressure into the stent graft was 140 mmHg or 18665.08 Pa and the velocity of the blood into the stents graft was assumed to be uniform and equal to a peak systolic flow rate of 0.60 m/s. Density was defined as 1060 kg/m^3, according the standard values cited in the literature. Blood was represented by the Navier–Stokes equation $\rho v \cdot \nabla v = -\nabla \cdot \tau - \nabla P$ [5] and continuity equation $\nabla \cdot v = 0$ [5] where v is the 3D velocity vector, P the pressure, r the density and τ the shear stress term. Carreau model was adopted for viscosity.[6,7]

The haemodynamic parameters that were assessed at the stented aorto-iliac bifurcation were static pressure (Pa), Reynolds number, vorticity magnitude (1/s), stream function (kg/s), strain rate (1/s), wall shear stress (Pa) and skin friction coefficient, as defined in the following. Pre- and post-stenting visual analysis was obtained also for the dynamic pressure (Pa), radial velocity (m/s), velocity magnitude (m/s), vorticity magnitude (m/s) and strain rate (1/s). The numeric grid was created from the geometry using ANSYS Meshing 14.0 (Ansys, Inc., Canonsburg, PA) while the simulations were conducted using the commercial software ANSYS FLUENT 14.0 (Ansys, Inc., Canonsburg, PA). The theoretical impact of the various fluid dynamic variables considered in the study on the development of stenosis and re-stenosis are listed in Table 1. Statistical analysis, in terms of level of significance (*P*-value), was not done because the results are reported as weighted-area average. In particular, given the study design, biomechanics results and the absence of a cohort population (sample size), traditional statistical tests such as t-test or chi-square cannot be performed.

Calculation

Static and dynamic pressure in the vessel were been evaluated in pascals. In particular, dynamic pressure has been defined as

$$q \equiv \frac{1}{2}\rho v^2$$

Cells Reynolds number, indicated in text as Reynolds number (Re), represents the local Reynolds number based

Table 1: Theoretical impact of the considered variables on the iliac arteries

Variables	Theoretical impact on the vessel
Static pressure	Associated with the proliferation of vascular smooth muscle cells
Dynamic pressure	Associated with a variation of the blood flow velocity, which has been linked to a higher risk of re-stenosis
Reynolds number (Re)	High Re number indicates a disturbed blood flow and is associated with a hemodynamic turbulence, which causes endothelial dysfunction and thrombogenicity.
Vorticity magnitude	High in the presence of a severe stenosis. A high vorticity magnitude, especially in a bifurcation lesion, affects both the blood flow velocity and vorticity, promoting endothelial dysfunction and/or thrombogenicity.
Stream function	Related to a change of the characteristic non-Newtonian fluid motion
Strain rate	Low levels have been related to an in-stent restenosis
Wall-shear	High Wall-shear stress plays a major role in both generation, progression and destabilisation of atherosclerotic plaques

on the velocity and the length scale of the calculation cell.[8,9] Wall shear stress (Pa) has been defined as the force that is tangentially acting on the surface due to friction. Vorticity magnitude represents the magnitude of the vorticity vector. Vorticity is a measure of the rotation of a fluid element as it moves in the domain, and it has been defined as the curl of the velocity vector. Stream function has been considered as the relationship between the streamlines and the statement of conservation of mass. Finally, skin friction coefficient has been considered as a non-dimensional parameter, which has been defined as the ratio of the wall shear stress and the reference dynamic pressure.

RESULTS

Profile of fluid parameters across different angles

In the physiologic model (without stenosis), across the different angles, static pressure, Reynolds number and stream function had lower values in 30° bifurcation angle with a gradient from 70° to 30° angles, whereas all the other parameters were inversely higher, suggesting that more spread is the angle, more turbulent and prone to plaque development is the bifurcation (Table 2). In the pathologic model, this trend was maintained with the difference that wall shear stress, vorticity magnitude and strain rate were higher in 45° and 30° compared to 70° bifurcation angle (Table 3 and Figure 2). A difference between right and left iliac artery and thus stenosis 1 and stenosis 2 is obviously due to the smaller take of angle on the left compared to the right iliac artery in human beings.

Profile of fluid parameters after stenting across different angles, kissing height and stent type

After stenting, all the fluid parameters decreased homogenously independent of the stent type (Table 4) maintaining a gradient in favour of 30° compared to 45° and 70° angles.

Comparing self-expandable and balloon-expandable stents and low to high kissing, a slightly different profile was observed across all angles for low kissing using self-expandable stents where Reynolds number, vorticity magnitude, stream function, strain rate, and wall shear stress were lower (Table 4).

Looking at the percentage deviation from the physiologic model (Table 5), the absolute greater deviation was observed for low kissing using self-expandable stents across all angles. In particular, the percentage deviation of wall shear stress seemed greater at 45° angle using high kissing and self-expandable stents, suggesting that high kissing using balloon-expandable stent might have a favourable profile at 30° and 70° angles, but high kissing using self-expandable stent might have the most favourable profile at 45° angle.

Table 2: Area weighted average analysis of the entire physiologic models among different Carrefour angle

	Physiologic Model		
	α=70°	**α=45°**	**α=30°**
Static pressure (Pa) [mmHg]	18759.02[140.69]	18734.96 [140.51]	18677.71 [140.08]
Reynold number	38.94	24.93	17.39
Vorticity magnitude (1/s)	892.50	1293.93	1437.32
Stream function (kg/s)	1.27	0.63	0.39
Strain rate (1/s)	912.17	1308.06	1450.0
Wall shear stress (Pa)	0.93	1.21	1.20
Skin friction coefficient	0.004	0.006	0.006

Table 3: Area weighted average analysis of the entire pathologic models among different Carrefour angle

	Pathologic model		
	α=70°	**α=45°**	**α=30°**
Static pressure (Pa) [mmHg]	19414.14	19180.85	19150.75
Reynold number	48.87	29.51	20.06
Stenosis 1	35.18	8.52	12.28
Stenosis 2	27.99	15.36	12.47
Vorticity magnitude (1/s)	1654.32	2448.30	2412.36
Stenosis 1	10077.59	16993.16	15228.56
Stenosis 2	11081.10	14052.73	13925.36
Stream function (kg/s)	1.65	0.78	0.51
Strain rate (1/s)	1753.83	2592.02	2480.50
Wall shear stress (Pa)	2.41	3.20	2.73
Stenosis 1	55.06	69.84	65.80
Stenosis 2	55.81	59.74	60.82
Skin friction coefficient	0.012	0.016	0.014

Table 4: Net area-weighted average comparison of fluid dynamic parameters

Angle and stenting techniques	Stent	Static pressure (Pa) [mmHg]	Reynolds number	Vorticity magnitude (1/s)	Stream function (kg/s)	Strain rate (1/s)	Wall shear (Pa)	Skin friction coefficient
α=70°								
High kissing	SE	18757.07[140.67]	38.17	881.63	1.25	900.85	0.92	0.004
	BE	18757.92[140.68]	38.58	884.58	1.26	904.04	0.92	0.004
Low kissing	SE	18754.77[140.66]	37.49	860.79	1.23	879.74	0.89	0.004
	BE	18755.89[140.66]	37.85	868.73	1.24	887.74	0.90	0.004
α =45°								
High kissing	SE	18733.86[140.50]	24.48	1271.44	0.62	1285.24	1.92	0.006
	BE	18734.34[140.50]	24.70	1282.66	0.63	1296.62	1.20	0.006
Low kissing	SE	18732.91[140.49]	24.04	1224.90	0.61	1262.46	1.16	0.006
	BE	18733.38[140.50]	24.26	1260.21	0.62	1273.84	1.18	0.006
α =30°								
High kissing	SE	18678.44[140.08]	17.08	1412.52	0.38	1425.92	1.18	0.006
	BE	18678.13[140.08]	17.23	1424.97	0.38	1438.47	1.19	0.006
Low kissing	SE	18679.71[140.09]	16.77	1387.90	0.37	1401.07	1.16	0.006
	BE	18678.83[140.09]	16.93	1400.19	0.38	1413.48	1.17	0.006

BE: balloon-expandable; SE: self-expandable.

Table 5: Percentage deviation from the physiologic values of fluid parameters after stenting

	Δ% α=70				Δ% α=45				Δ% α=30			
	HK		LK		HK		LK		HK		LK	
	SE	BE	SE	BE	SE	BE	SE	BE	SE	BE	SE	BE
Static pressure (Pa)	0.01	0.01	0.02	0.02	0.01	0.00	0.01	0.01	0.00	0.00	0.01	0.01
Reynolds number	1.98	0.92	3.72	2.80	1.81	0.92	3.57	2.69	1.78	0.92	3.57	2.65
Vorticity magnitude (1/s)	1.22	0.89	3.55	2.66	1.74	0.87	3.47	2.61	1.73	0.89	3.44	2.58
Stream function (kg/s)	1.57	0.79	3.15	2.36	1.59	0.0	3.17	1.59	2.56	2.56	5.13	2.56
Strain rate (1/s)	1.21	0.89	3.57	2.68	1.74	0.84	3.49	2.62	1.66	0.80	3.37	2.52
Wall shear (Pa)	1.08	1.08	4.30	3.23	5.68	0.83	4.13	2.48	1.67	0.83	3.33	2.50
Skin friction coefficient	0.0	0.0	0.0	0.0	0.0	0.0	0.0	0.0	0.0	0.0	0.0	0.0

BE: balloon-expandable; HK: High kissing; LK: Low kissing; SE: self-expandable.

DISCUSSION

Our non-invasive evaluation seems to suggest that physiologically more spread is the aortoiliac bifurcation angle, more turbulent and prone to plaque development is the bifurcation itself. In the pathologic model, this trend is maintained with the difference that wall shear stress, vorticity magnitude and strain rate were higher in 45° and in 30° compared to 70° angle.

When a stent technique is to be applied, high kissing using balloon-expandable stent might have a favourable profile at 30° and 70° angles, but high kissing using self-expandable stent might have the most favourable profile at 45° angle. Obviously, whether these results impact the clinical outcomes of each technique is beyond the scope of this study, and clinical randomized studies are necessary to confirm these hypotheses.

However, we can generally argue that reconstructing the aortic carrefour in higher position might result in a more physiological fluid dynamic profile. In our analysis, we choose self-expandable and balloon-expandable stents because they are the most widely used in our centre as well as in the rest of the country. As it is known, it is extremely difficult to propose a stent with the best ideal properties. However, both self- and balloon-expandable stents currently represent the widely used intravascular device in the treatment of aortoiliac occlusive disease. Our results seem to fit well if we take in account the current treatment

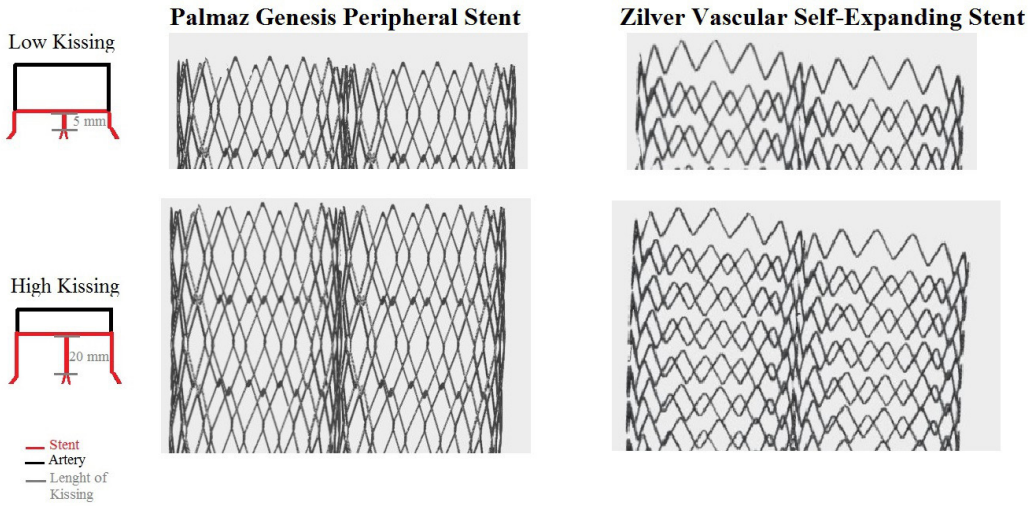

Figure 3: Schematic representation of the height of kissing applied to the analysis. Arterial walls have been subtracted to better represent the stent interactions.

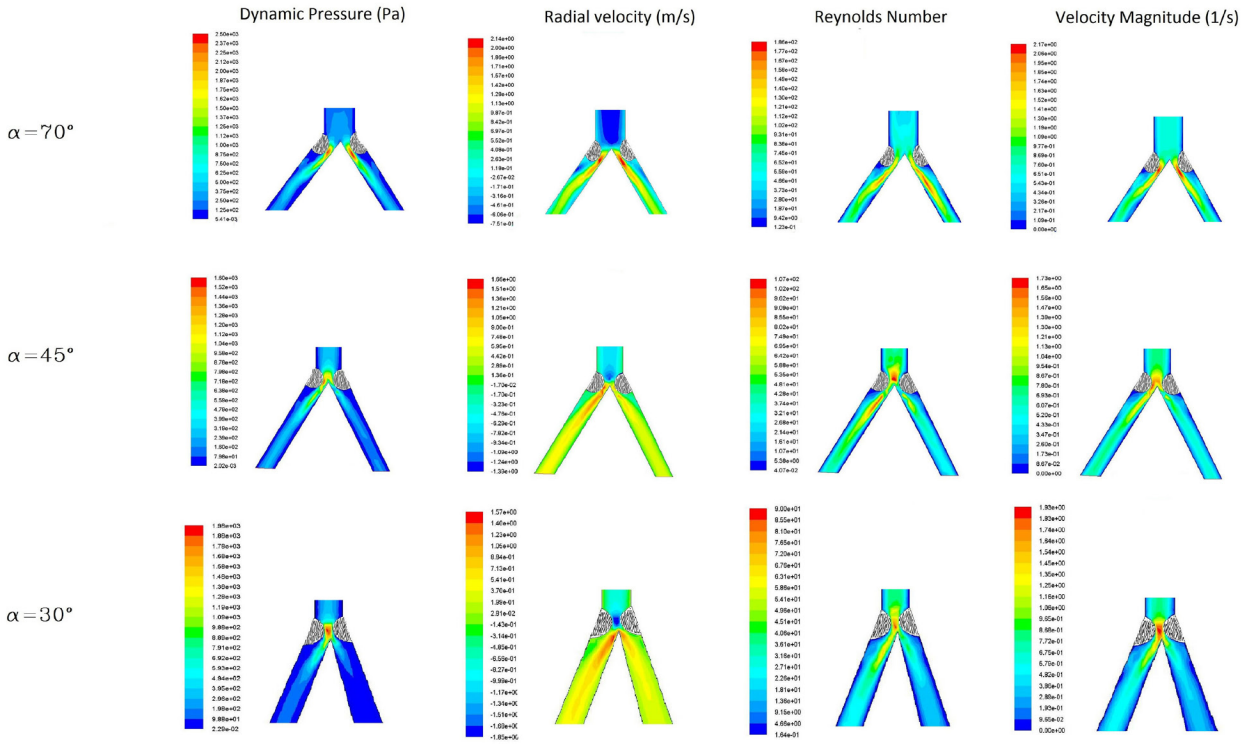

Figure 4: Profile of the stenosis on the iliac artery bifurcation model in respect to the different fluid parameters considered in the analysis.

of abdominal aortic aneurysm (AAA), a field recently well investigated with CFD.[10] During endovascular AAA repair, the aorto-iliac bifurcation is generally reconstructed in a very high position with respect to the anatomic normal position and this technique seems to have no impact or a beneficial impact on fluid dynamic[11, 12] in the iliac and femoral vessels.

High Reynolds number and low wall shear stress have been correlated along with vorticity magnitude to the development of atherosclerotic plaque [13, 14]: the effects on development of stent thrombosis or restenosis is less clear, but makes good sense to avoid altering the fluid dynamic too much and to preserve the flow distal to the stented vessel from fluid dynamic disturbances prone to plaque development. As known, Re is a dimensionless parameter, that is, the ratio of inertia forces to viscous forces. On a more practical view, disturbed laminar flow is prone to occur in vascular segment with high Reynolds number.[15] As well known, at least in the most studies of

vessels, that is the coronary arteries, low wall shear stress is related to the development of greater plaques and necrotic core progression with a constrictive remodelling whereas high wall shear stress segment develops greater necrotic core and calcium progression with expansive remodelling.

The comparison of self-expandable and balloon expandable stents is less relevant to be discussed. Traditionally focal bilateral stenosis was more precisely treated by balloon-expandable stent, in particular for the capability of such device to be exactly positioned at the common iliac ostia.[16] With the current technology, self-expandable stents are more widely used nowadays, but amount of calcium, stenosis length and vessel diameter obviously influence the choice between self-expandable and balloon-expandable stent.[17,18] Using a high kissing and reconstructing the aorto-iliac bifurcation in a higher position increases the possibility of choosing self-expanding stents over balloon-expandable stent.

Our analysis seems to suggest that for angle approximately 45° (in our institution the more frequent angle), high kissing using self-expandable stent might be the theoretically more physiologic option, while for angle approximately 30° and 70° angles, high kissing with balloon-expandable or self-expandable stent provide almost the same fluid dynamic profile. Although the real impact in the clinical real-world of different techniques, a stents cannot be retrieved by this study, but based on these data to avoid low kissing appears to be a more physiologic option.

LIMITATIONS

Our study takes into account an ideal aorto-iliac bifurcation models. The vessels have been considered non-compliant, straight and stationary. Our model considered an optimal stent deployment without residual stenosis despite in daily clinical practice, the different angles, the amount and circumferential extent of the calcium, the length of the respective lesion, and many other parameters have an obvious impact on the implantation technique and outcomes. Moreover, the imposed hemodynamic conditions assume that the patient was hemodynamically stable. Other limitations of the study are that we did not evaluate the time-averaged wall shear stress (TAWWS), oscillatory index (OSI) and the relative residence time, which had a recognized role in the treatment, for example, of coronary artery stenosis.

CONCLUSIONS

Bifurcation angles impact both the physiologic and pathologic models. In the same way, different stent types and configurations seem to impact the local fluid dynamic. High kissing appears to be more favourable in respect of the aortic Carrefour, in particular at 45° angle, than low kissing.

CFD, being able to be derived both from computed tomography scan or invasive angiography, appears to be an ideal tool to predict fluid dynamic profile before and after stenting in aortoiliac bifurcation.

Conflict of Interest

None of the other authors have identified a conflict of interest.

REFERENCES

1. Deswal A, Tamang BK, Bala A. Study of aortic- common iliac bifurcation and its clinical significance. J ClinDiagn Res 2014; 8:AC06-8.
2. Timothy C, Rigatelli G, Cardaioli P, Rosli Mohd A, Nanjiundappa A. Iliac artery stenosis. In: Practical handbook of Advanced Interventional Cardiology. Tips and Triks, 4th edition. US: Wiley-Blackwell, 2013; 579-603.
3. Zuin M, Rigatelli G, Faggian G, Roncon L. Mathematics and Cardiovascular Interventions: Role of the Finite Element Modeling in Clinical Decision Making. JACC Cardiovasc Interv 2016; 9:507-8.
4. Rigatelli G, Zuin M, Dell'Avvocata F, Vassilev D, Daggubati R, Nguyen T, *et al.* Evaluation of coronary flow conditions in complex coronary artery bifurcationsstenting using computational fluid dynamics: Impact of final proximaloptimization technique on different double-stent techniques. Cardiovasc Revasc Med 2017; 18:233-40.
5. Cho YI, Kensey, K.R. Effects of the non-Newtonian viscosity of blood on flows in a diseased arterial vessel. Part 1: steady flows. Biorheology 1991; 28: 241–62.
6. Katritsis DG, Theodorakakos A, Pantos I, Gavaises M, Karcanias N, Efstathopoulos EP. Flow patterns at stented coronary bifurcations: computational fluid dynamics analysis. Circ Cardiovasc Interv 2012; 5:530-9;
7. Johnston BM, Johnston PR, Corney S, Kilpatrick D. Non-Newtonian blood flow in human right coronary arteries: steady state simulations. J Biomech 2004; 37:709-20.
8. Nichols WW, O'Rourke MF. The nature of flow of a liquid. *In* McDonald's Blood Flow in Arteries: Theoretical, Experimental and Clinical Principles. 4th ed. Arnold, London, U.K. 1998: 11–53.
9. Karino T, Goldsmith HL, Motomiya M, Mabuchi S, Sohara Y. Flow patterns in vessels of simple and complex geometries. Ann N Y Acad Sci 1987; 516: 422–41.
10. Li Z, Kleinstreuerb C. Blood flow and structure interactions in a stented abdominal aortic aneurysm model. Med Eng Phys 2005; 27:369-82.
11. Soudah E, Ng EY, Loong TH, Bordone M, Pua U, Narayanan S. CFD modelling of abdominal aortic aneurysm on hemodynamic loads using a realistic geometry with CT. Comput Math Methods Med 2013; 2013:472-564.
12. GrootJebbink E, Grimme FA, Goverde PC, van Oostayen JA, Slump CH, Reijnen MM. Geometrical consequences of kissing stents and the Covered Endovascular Reconstruction of the Aortic Bifurcation configuration in an in vitro model for endovascular reconstruction of aortic bifurcation. J Vasc Surg 2015; 61:1306-11.
13. Frauenfelder T, Lotfey M, Boehm T, Wildermuth S. Computational fluid dynamics: hemodynamic changes in abdominal aortic aneurysm after stent-graft implantation. Cardiovasc Intervent Radiol 2006; 29:613-23.
14. Liu B, Tang D. Computer simulations of atherosclerotic plaque growth in coronary arteries. Mol Cell Biomech 2010; 7:193-202.
15. LaMack JA, Himburg HA, Li XM, Friedman MH. Interaction of wall

shear stress magnitude and gradient in the prediction of arterial macromolecular permeability. Ann Biomed Eng 2005; 33:457-64.
16. Aggarwal V, Waldo SW, Armstrong EJ. Endovascular revascularization for aortoiliac atherosclerotic disease.Vasc Health Risk Manag 2016; 12:117-27.
17. Moon JY, Hwang HP, Kwak HS, Han YM, Yu HC. The Results of Self-Expandable Kissing Stents in Aortic Bifurcation. Vasc Specialist Int 2015; 31:15-9.
18. Sabri SS, Choudhri A, Orgera G, Arslan B, Turba UC, Harthun NL, *et al.* Outcomes of covered kissing stent placement compared with bare metal stentplacement in the treatment of atherosclerotic occlusive disease at the aorticbifurcation. J Vasc Interv Radiol 2010; 21:995-1003.

How to cite this article: Rigatelli G, Zuin M, Dell'Avvocata F, Nanjundappa A, Daggubati R, Nguyen T. Non-invasive evaluation of fluid dynamic of aortoiliac atherosclerotic disease: Impact of bifurcation angle and different stent configurations. J Transl Intern Med 2018; 6: 138-45.